Original Article

Molecular Syndromology

Mol Syndromol
DOI: 10.1159/000491567

Published online: July 21, 2018

An FDA-Approved Drug Screen for Compounds Influencing Craniofacial Skeletal Development and Craniosynostosis

Marian Seda[a] Maartje Geerlings[a] Peggy Lim[a] Jeshmi Jeyabalan-Srikaran[a]
Ann-Christin Cichon[b] Peter J. Scambler[b] Philip L. Beales[a]
Victor Hernandez-Hernandez[a] Andrew W. Stoker[b] Dagan Jenkins[a]

[a]Genetics and Genomic Medicine, and [b]Developmental Biology and Cancer Programmes, UCL Institute of Child Health, London, UK

Keywords
FDA-approved drug screen · Neural crest stem/progenitor cells · Skeletal development

Abstract
Neural crest stem/progenitor cells (NCSCs) populate a variety of tissues, and their dysregulation is implicated in several human diseases including craniosynostosis and neuroblastoma. We hypothesised that small molecules that inhibit NCSC induction or differentiation may represent potential therapeutically relevant drugs in these disorders. We screened 640 FDA-approved compounds currently in clinical use for other conditions to identify those which disrupt development of NCSC-derived skeletal elements that form the zebrafish jaw. In the primary screen, we used heterozygous transgenic *sox10:gfp* zebrafish to directly visualise NCSC-derived jaw cartilage. We noted partial toxicity of this transgene in relation to jaw patterning, suggesting that our primary screen was sensitised for NCSC defects, and we confirmed 10 novel, 4 previously reported, and 2 functional analogue drug hits in wild-type embryos. Of these drugs, 9/14 and 7/14, respectively, are known to target pathways implicated in osteoarthritis pathogenesis or to cause reduced bone mineral density/increased fracture risk as side effects in patients treated for other conditions, suggesting that our screen enriched for pathways targeting skeletal tissue homeostasis. We selected one drug that inhibited NCSC induction and one drug that inhibits bone mineralisation for further detailed analyses which reflect our initial hypotheses. These drugs were leflunomide and cyclosporin A, respectively, and their functional analogues, teriflunomide and FK506 (tacrolimus). We identified their critical developmental windows of activity, showing that the severity of defects observed related to the timing, duration, and dose of treatment. While leflunomide has previously been shown to inhibit NCSC induction, we demonstrate additional later roles in cartilage remodelling. Both drugs altered expression of extracellular matrix metalloproteinases. As proof-of-concept, we also tested drug treatment of disease-relevant mammalian cells. While leflunomide treatment inhibited the viability of several human NCSC-derived neuroblastoma cell

KARGER

E-Mail karger@karger.com
www.karger.com/msy

Dagan Jenkins
Genetics and Genomic Medicine
UCL Institute of Child Health
30 Guilford Street, London WC1N 1EH (UK)
E-Mail d.jenkins@ucl.ac.uk

lines coincident with altered expression of genes involved in ribosome biogenesis and transcription, FK506 enhanced murine calvarial osteoblast differentiation and prevented fusion of the coronal suture in calvarial explants taken from Crouzon syndrome mice.

Craniosynostosis, premature fusion of sutures within the skull at birth, is a relatively common and serious condition affecting approximately 1 in 2,100 children [Hehr and Muenke, 1999; Wilkie et al., 2010]. A major focus of research into craniosynostosis is to identify drug treatments to improve outcomes following corrective surgery for this condition. The calvarium (or skull vault) forms through the process of intramembranous ossification [Twigg and Wilkie, 2015]. The cranial sutures are the major site of new bone formation within the skull, where osteoblasts form bone directly within the mesenchyme without the need for a cartilage anlagen. In simple terms, the formation of new bone and maintenance of suture patency is driven by the balance between osteoblast proliferation and differentiation. As such, osteoblasts have long been considered an obvious target for chemical therapies for craniosynostosis. However, cultured chick and rodent calvarial mesenchyme expresses chondrocyte-specific collagen isoforms and can differentiate into both osteoblasts and chondrocytes, and small islands of cartilage can form within the cranial sutures [Aberg et al., 2005]. Therefore, calvarial mesenchyme has been proposed to have dual osteoblast and chondrogenic identity. The finding of mutations in interleukin genes in syndromes featuring immunodeficiency, failed molar tooth eruption, and craniosynostosis also suggests the involvement of bone-resorbing osteoclasts in maintenance of suture patency [Nieminen et al., 2011; Keupp et al., 2013; Schwerd et al., 2017]. Therefore, several key bone cell types are potentially relevant targets for treatment of craniosynostosis.

Neural crest stem/progenitor cells (NCSCs) are a transient population of embryonic multipotent stem cells that are induced at the lateral margins of the neural plate and migrate extensively to populate a variety of tissues. Several lines of evidence suggest that NCSC patterning defects cause craniosynostosis. Within the skull, NCSCs have been shown to make a significant contribution to the frontal bones of the skull and the sagittal suture, but they make no contribution whatsoever to the parietal bone or coronal suture [Jiang et al., 2002]. *Twist* mutant mice exhibit coronal craniosynostosis with mislocalisation of NCSCs within the coronal sutures and parietal bone [Merrill et al., 2006]. Knockout of the *Msx2* gene, which drives osteoblast differentiation within the skull, rescued these defects, leading to proposal of a model whereby ectopic localisation of NCSCs to the coronal suture and parietal bone leads to enhanced osteoblast differentiation. Ephrin signalling is known to regulate NCSC migration, and thus heterozygosity for *EFNB1* mutations in craniofrontonasal syndrome have been suggested to cause craniosynostosis secondary to cellular interference and NCSC migration defects in female foetuses (it should be noted, however, that EFNB1 has also been shown to regulate osteoblast differentiation directly) [Twigg et al., 2004, 2006, 2013; Babbs et al., 2011; Cheng et al., 2013]. Engrailed 1 (*En1*) has also been identified as a necessary regulator of cell movement and neural crest/mesoderm lineage boundary positioning during coronal suture formation [Deckelbaum et al., 2012]. Given these findings, we hypothesised that drugs which inhibit NCSC identities or their subsequent differentiation/remodelling could be therapeutically relevant in craniosynostosis.

The zebrafish has emerged as a powerful model organism for in vivo drug screening [Wiley et al., 2017]. As a vertebrate model, it presents several key advantages including large clutch size and fecundity, external embryonic development, visual transparency, and genetic tractability (although recent results from reverse genetics suggest that the zebrafish has become redundant as a genetic model owing to compensatory mechanisms and gene redundancy). Oxygen also diffuses freely into zebrafish embryos, which is a key advantage, allowing embryos to survive drug treatments that can frequently disrupt cardiovascular system formation. While zebrafish embryos develop rapidly, their subsequent growth and maturation is relatively much slower. In particular, the membranous bones of the skull vault do not ossify over the brain until the second month of life, thereby precluding drug screens based on calvarial development in this organism [Mork and Crump, 2015].

An important consideration relates to drug screen design, which generally falls into 1 of 2 camps. One option is a "modifier" screen, whereby a faithful (typically genetic) model of disease is treated with drugs in an attempt to ameliorate a disease phenotype. A second option that we will refer to as a "perturbation" screen involves the testing of drugs for their ability to generate a phenotype in otherwise wild-type/normal animals. This approach requires careful selection of a cell type that is relevant to a disease and analysis of a specific marker of these cells in order to identify drugs that are therapeutic. Perturbation

screens can also allow investigation of drug teratogenicity. For example, many drugs are known to disrupt craniofacial/skeletal development and tissue homeostasis as side effects, e.g., association between valproate ingestion during pregnancy and craniosynostosis [Twigg and Wilkie, 2015]. Clearly, perturbation screens would require subsequent validation/follow-up in a (mammalian) disease-relevant model. Given that perturbation screens are disruptive in their design, they have the advantage of being less sensitive to genetic threshold effects and buffering mechanisms within a network than modifier screens, and may therefore be more transferrable across species.

While perturbation screens may seem counterintuitive in terms of therapy, this approach has proved to be highly productive, whereas the published evidence has demonstrated the modifier approach to be far less successful. Approximately 30 unbiased in vivo drug screens using zebrafish have been reported to date to our knowledge, and all but 4 of these were based on the perturbation design [Peterson et al., 2004; Stern et al., 2005; North et al., 2007; Kitambi et al., 2009; Ishizaki et al., 2010; Paik et al., 2010; Rihel et al., 2010; Ni et al., 2011; Peal et al., 2011; Rovira et al., 2011; Namdaran et al., 2012; Ridges et al., 2012; Gut et al., 2013; Le et al., 2013; Kong et al., 2014; Mork and Crump, 2015]. This suggests a reporting bias such that most of the many modifier screens that we know to have been conducted in the field have not yielded any hits. Of 4 published modifier screens, an average confirmed drug hit rate of 0.086% (range 0.17–0.06%) was reported [Peterson et al., 2004; Stern et al., 2005; Paik et al., 2010; Peal et al., 2011], whereas for perturbation screens that reported their results in full, an average confirmed hit rate of 2.50% (range 8.2–0.08%) was achieved [North et al., 2007; Kitambi et al., 2009; Ishizaki et al., 2010; Rihel et al., 2010; Ni et al., 2011; Rovira et al., 2011; Namdaran et al., 2012; Ridges et al., 2012; Gut et al., 2013; Le et al., 2013; Kong et al., 2014; Mork and Crump, 2015]. Thus a typical screen of 1,000 small molecules, which is achievable in most labs using nonautomated zebrafish screens, is expected to produce 25 hits in a perturbation screen but none in a modifier screen. Clearly, there is also likely to be a significant rate of attrition in transferring suitable drug hits to mammalian systems for treatment of disease, and so a number of hits are likely to be required for a realistic chance of translation.

The zebrafish viscerocranium is derived from NCSCs that contribute to the 7 pharyngeal arch derivatives, including the mandible/Meckel cartilages and the pterygoid/ethmoid plate complex, which constitute the most anterior aspects of the lower and upper jaw, respectively [Schilling and Kimmel, 1997; Mork and Crump, 2015]. The lower jaw consists of 7 paired and bilaterally symmetric cartilage elements. In anteroposterior sequence, these include Meckel cartilage, the ceratohyoid cartilage and arches 3–7 which consist of ceratobranchials attached to hypobranchials. These elements are arranged in a stereotypical pattern and are composed of chondrocytes that first emerge during the third day post-fertilisation (dpf). These cells are derived from cranial NCSCs that are first induced in the neural plate border at the earliest somite stages and subsequently migrate through the branchial arches. Failed NCSC induction prevents formation of this cartilage, and many zebrafish models of abnormal patterning/migration of NCSCs have been shown to exhibit quantitative increases in the angle between the paired cartilage elements and particularly the ceratohyoid cartilages. Once formed, these cartilage elements are remodelled through convergent extension cell movements of chondrocytes, enzymatic regulation of extracellular matrix glycosaminoglycans, and cellular hypertrophy. Both osteoblasts and osteoclasts localise throughout the zebrafish jaw at these stages or shortly afterwards [Eames et al., 2013; Sharif et al., 2014; Mork and Crump, 2015]. Anatomically, this manifests as a progressive reduction in the angle between the ceratohyoids and the other branchial arch cartilages between 3–5 dpf.

Here, we report a drug screen of FDA-approved compounds that disrupt ceratohyoid cartilage formation in a perturbation screen. We report a hit rate consistent with published perturbation screens, and we enrich for novel "hits" that target skeletal tissue homeostasis. Our results demonstrate the importance of sustained drug treatment, which might be necessary to overcome compensatory mechanisms and could have relevance in future clinical translation. As proof-of-concept, we demonstrate possible efficacy of 2 compounds in mammalian ex vivo models of disease, including treatment of craniosynostosis.

Materials and Methods

Zebrafish

Zebrafish (*Danio rerio*) embryos were obtained from a wild-type strain and raised at 28.5°C in accordance with Home Office licence PPL 70/7892. Heterozygous *sox10:gfp* zebrafish were crossed to wild types to produce heterozygous embryos. Embryos were cultured in 24-well plates (3 per well) and treated with one of 640 FDA-approved drugs from the Enzo BML-2842 (v1.5) library, from mid- to late-gastrulation (8 hours post-fertilisation; hpf) until 5 dpf, at which stage NCC-derived craniofacial cartilage was imaged. Drugs stocks were stored at –80°C at 10 mM in DMSO. For drug treatments, small molecules were defrosted at 37°C and

diluted to 10 μM in E3 medium. In the secondary screen, putative drug hits were re-tested on >10 *sox10:gfp* heterozygotes, and in the tertiary screen, hits were tested on wild-type zebrafish stained using Alcian blue. In situ hybridisation was performed by standard techniques, using RNA probes labelled with digoxigenin (Roche) and detected using NBT/BCIP (Sigma). We note that, in order to aid visualisation of cartilage elements in Figure 4 only, PTU treatment was used in this particular experiment. However, throughout our drug screen and in subsequent analyses, PTU was not used, as this has been shown to sensitise zebrafish to jaw patterning defects through dysregulated retinoic acid signalling. Findings in this experiment were confirmed in parallel in embryos not treated with PTU.

Neuroblastoma Cell Culture

Neuroblastoma cell lines SK-N-AS, SK-N-SH, IMR32, and LAN5 are derived from the neural crest lineage within the adrenal gland. Cells were cultured in RPMI medium and 10% fetal calf serum, except for SK-N-SH which used MEME medium plus 10% fetal calf serum. Cells have been STR genotyped by ATCC or by the group of Frank Speleman, University of Ghent. For cell proliferation assays with leflunomide or teriflunomide, between 10,000 and 20,000 cells were plated per well in 96-well plates, and these were grown in the presence or absence of chemicals for 3 days, before being processed with Cell Cycle Kit-8 as per manufacturer's protocol (Sigma Aldrich). Absorbance values were measured at OD450nm and background (no cells) values subtracted before normalisation against untreated samples.

RNAseq and Analysis

The stranded total RNA libraries were prepared in accordance to the Illumina TruSeq Stranded mRNA Sample Preparation (October 2013 Rev E.) for Illumina Paired-End Multiplexed Sequencing. Poly-A mRNA in the tRNA samples were first purified using Illumina poly-T oligo-attached magnetic beads and 2 rounds of purification. During the second elution of the poly-A RNA, the mRNA were also fragmented and primed with random hexamers for cDNA synthesis. Cleaved RNA fragments that were primed with random hexamers were reverse transcribed into first strand cDNA using reverse transcriptase and random primers followed by second strand cDNA synthesis. A single "A" nucleotide is added to the 3′ end of the blunt fragments to prevent ligating to one another during adapter ligation reaction. The adapters and indexes are ligated to the end of the double-stranded cDNA to prepare the sample for hybridisation onto a flow cell. The sample is then PCR amplified through 15 cycles of PCR to select samples that have the adapter molecules present on both ends of the DNA. The libraries were validated on the Agilent BioAnalyser 2100 to check the size distribution of the libraries and on the Qubit High Sensitivity to check the concentration of the samples. The pool was then loaded at a concentration of 8 pM onto 1 lane of an Illumina HiSeq2000 flow cell v3. Samples were sequenced using 100 bp SE runs. KEGG pathway gene ontology terms statistically significantly enriched within the list of differentially expressed genes ($\log_2$-fold change >2; $p < 0.05$) while identified according to DAVID software analysis (https://david.ncifcrf.gov/).

Calvarial Explant Culture

We tested FK506 for rescue of craniosynostosis in a calvarial explant system that we and others have developed using Crouzon mice [Eswarakumar et al., 2006]. Heterozygous stud males carrying the *Fgfr2*^{C342Y} mutation were crossed with wild-type females on a CD-1 genetic background. Typically 8–12 pups were produced, with an expected 50:50 ratio of heterozygotes and wild types. Pups were sacrificed at embryonic day (E) 18.5. Skin was removed from the scalp, the skull base was dissected and this and the brain were discarded. No attempt to remove dura or other tissue was made. Explants were cultured in one well of a 12-well plate in 2 mL of DMEM F12 medium (Gibco) supplemented with 10% fetal bovine serum. Explants were cultured for 14 days. Media was changed every 2 days and included 100 nM FK506 dissolved in DMSO, or DMSO alone, as a control. Differentiation of primary osteoblasts derived from wild-type CD-1 calvarial from 4-day-old mice and grown for 14 days.

Primary Osteoblast Culture

Primary mouse osteoblastic cells were obtained by sequential enzyme digestion of excised calvarial bones from 4-day-old CD1 mice using a 3-step process (1% trypsin in PBS for 10 min, 0.2% collagenase type II in Hanks balanced salt solution (HBSS) for 30 min, and 0.2% collagenase type II in HBSS for 60 min). The first 2 digests were discarded and the cells resuspended in MEM supple-

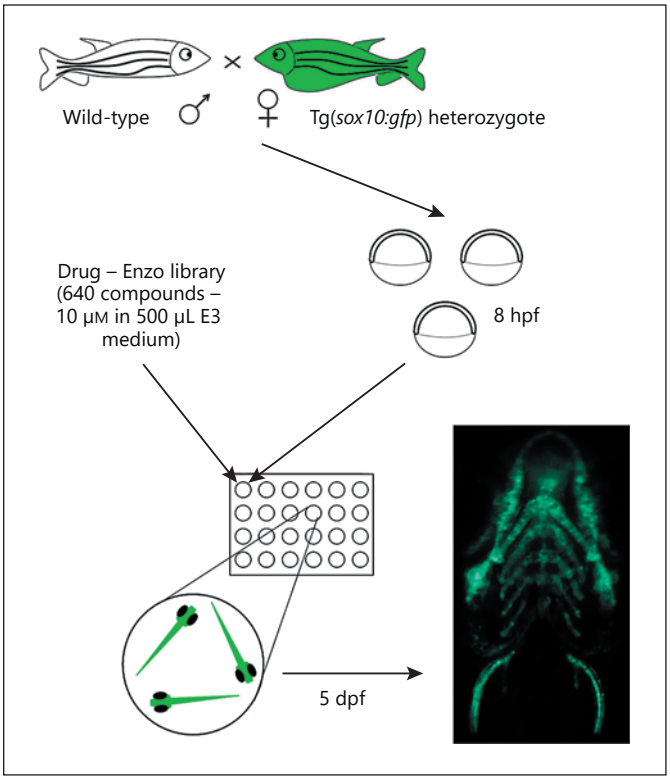

Fig. 1. Overview of zebrafish drug screen employed in this study. Three embryos from a wild-type x *sox10:gfp* heterozygote cross per well were treated with one of 640 FDA-approved drugs in a 24-well plate format from 8 hours post-fertilisation (hpf) and screened for quantitative increases in the angle of the ceratohyoid cartilage or gross malformations at 5 days post-fertilisation (dpf).

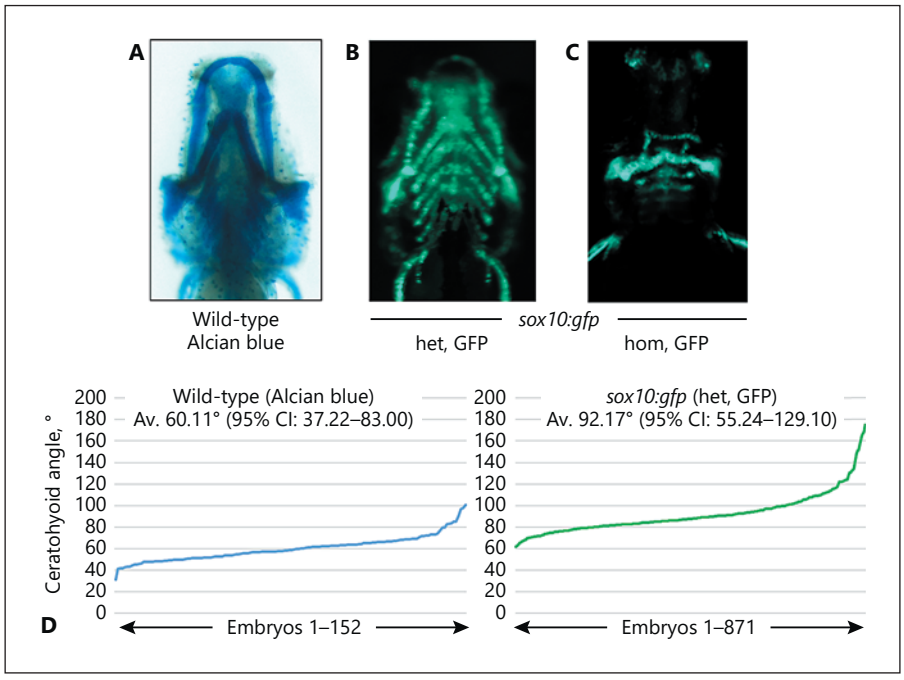

Fig. 2. *sox10:gfp* transgenic embryos are sensitised for jaw patterning defects. **A–C** Ventral views of wild-type zebrafish (**A**) or fry that are heterozygous (**B**) or homozygous (**C**) for the *sox10:gfp* transgene. Note the gross structural abnormalities in homozygotes. **D** Angles between the ceratohyoid cartilages for each of the 152 wild-type zebrafish (left) and 871 heterozygous transgenics (right) at 5 days post-fertilization. Av, average; CI, confidence interval; GFP, green fluorescent protein; hom, homozygous; het, heterozygous.

mented with 10% FCS, 2 mM L-glutamine, 1% gentamicin, 100 U/mL penicillin, 100 µg/mL streptomycin and 0.25 µg/mL amphotericin. Cells were cultured for 2–4 days at 37°C in 5% CO_2 until they reached confluence. They were then cultured in 6-well trays in MEM supplemented with 2 mM β-glycerophosphate and 50 µg/mL ascorbic acid, with half medium changes every 3 days. FK506 (0, 0.001, 0.01, 0.1, 1, and 10 nM) was added to the culture every 3 days from day after seeding. Total RNA were extracted from cells at day 14 (differentiating osteoblasts) using TRIzol® reagent (Thermo Fisher) according to manufacturer's instructions.

cDNA was reverse-transcribed from 1 µg of total RNA using Omniscript RT kit (Qiagen). Real-time qPCR was carried out using iTaq™ Universal SYBR Green supermix (Bio-Rad) with primers for the mouse *Hprt* (forward, GCAGTACAGCCCCAAAATGG; reverse, AACAAAGTCTGGCCTGTATCCAA), *Col1A1* (forward, GGTCCTCGTGGTGCTGCT; reverse, ACCTTTGCCCCCTTCTTTG), *Alp* (forward, GATAACGAGATGCCACCAGAGG; reverse, TCCACGTCGGTTCTGTTCTTC), *Osx* (forward, ATGGCGTCCTCTCTGCTTG; reverse, TGAAAGGTCAGCGTATGGCTT), and *Runx2* (forward, GACTGTGGTTACCGTCATGGC; reverse, ACTTGGTTTTTCATAACAGCGGA) genes.

Results

A Sensitised Screen for FDA-Approved Drugs Targeting Craniofacial Neural Crest

Given that abnormal location of NCSCs within the coronal suture or parietal bone has been proposed to drive ectopic osteoblast differentiation and cranial suture fusion, we hypothesised that small molecules that inhibit NCSC induction or their subsequent differentiation could be therapeutically relevant in craniosynostosis. Following the rationale outlined above, we designed a perturbation screen using *sox10:gfp* transgenic zebrafish in which green fluorescent protein (GFP) expression is driven by 4.9 kb of the zebrafish *sox10* promoter/upstream sequence [Dutton et al., 2008]. In this line, neural crest-derived craniofacial cartilage making up the jaw is labelled with GFP, allowing direct visualisation of these structures in live embryos (Fig. 1). During the course of our initial studies, we noticed that one quarter of fry from an incross of *sox10:gfp* heterozygotes demonstrated severe abnormalities of the jaw, including a strong reduction in Meckel cartilage and severe widening of the ceratohyoids and ceratobranchials (Fig. 2A–C), suggesting that the transgene is toxic to NCSC patterning when homozygous. We therefore included only heterozygous transgenic zebrafish in our screen by crossing heterozygous females with wild-type males. We included 3 fish per well in a 24-well plate format. On average, 50% of fry were heterozygous and could therefore be analysed in our screen.

In the primary screen, the effects of 640 FDA-approved drugs were tested by treating embryos from 8 hpf [equating to approximately 50% epiboly (E50)] to avoid defects in early cell division or gastrulation, until 5 dpf when ev-

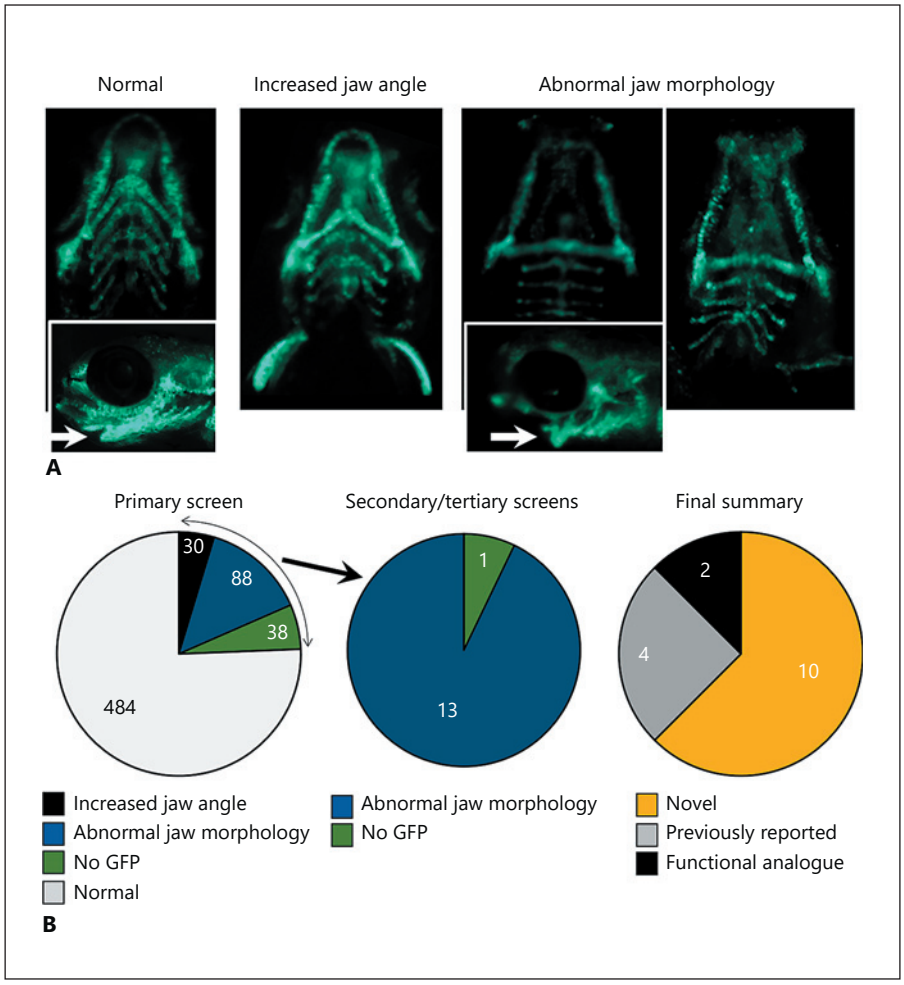

Fig. 3. Drug screen results. **A** Examples of morphological phenotype categories identified in the screen, in comparison to normal control zebrafish. **B** Summary statistics of the number of drugs represented by each category in each of the 4 stages of screening/re-testing.

ery embryo was manually photographed (Fig. 1). Embryos were treated with a standard 10 μM dose of each of 640 compounds from the Screen-Well® FDA-approved drug library (Enzo, BML-2842 version 1.5) in E3 medium. This is a dose at which most bioactive compounds have been shown to be effective [Rennekamp and Peterson, 2015]. Measurement of the ceratohyoid jaw angle in the 871 heterozygous transgenic animals that were included in our primary screen revealed an average angle of 92.17°, whereas wild-type embryos stained for Alcian blue had an average angle of 60.11° (Fig. 2D). Not a single transgenic animal exhibited an angle as low as the average value for wild types. This suggests that the *sox10:gfp* transgene is therefore partially toxic in heterozygotes, and that our screen was sensitised for NCSC patterning defects.

In the primary screen, we identified 3 categories of candidate hits (Fig. 3A). This included drugs that were associated with: (i) a quantitatively increased angle between the ceratohyoid cartilages as a purely objective measure, (ii) gross morphological defects, or (iii) no GFP expression. Given the breeding scheme used, the latter would be expected in 12.5% of embryo trios by chance alone. In total, 156 putative hits were identified in the primary screen, including 30, 88, and 38 of categories i, ii, and iii, respectively (Fig. 3B). In a secondary screen, these compounds were each re-tested on approximately 10 transgenic animals, and reproducible hits here were tested in a tertiary screen for their effects on wild-type zebrafish that were stained for Alcian blue. Of the 640 compounds screened, 14 (2.2%) had reproducible effects on craniofacial cartilage in all 3 screens (Fig. 3, 4, and data not shown). We also re-ordered each of the 14 drugs that caused consistent phenotypes across all 3 screens from independent sources and tested them to exclude artefacts relating to chemical batch. Ten of these compounds were novel hits, having not previously been reported to affect

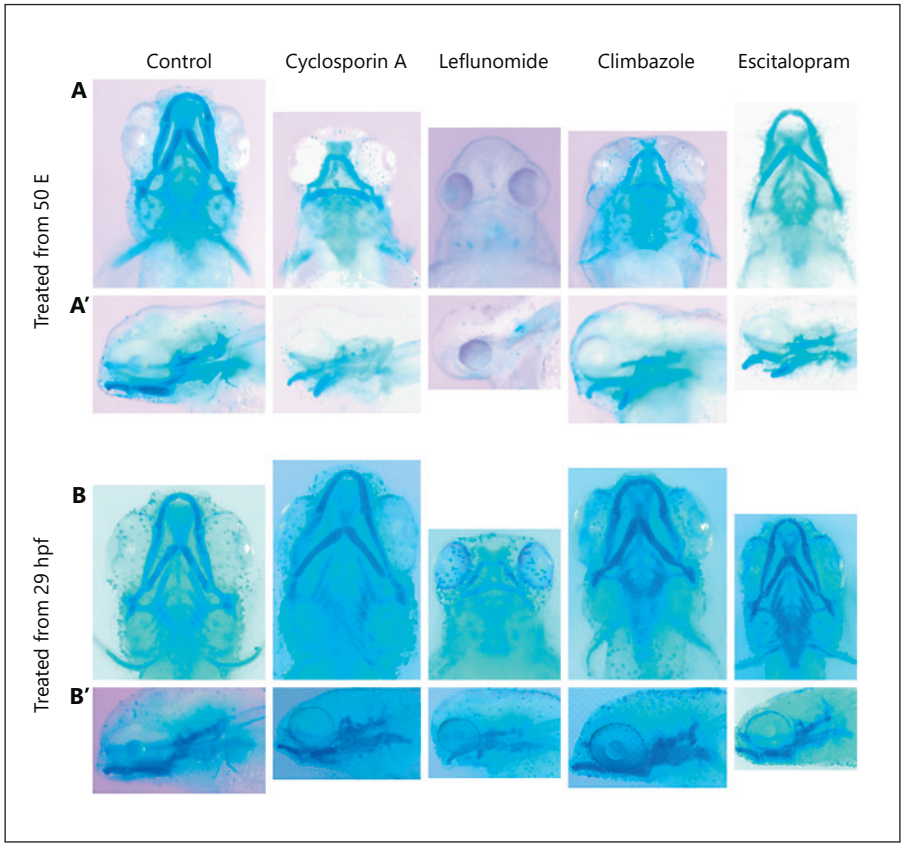

Fig. 4. Examples of drug re-testing on wild-type zebrafish. Alcian blue-stained zebrafish at 5 days post-fertilisation showing jaw cartilage following drug treatment from embryonic day (E) 50 (**A**, **A′**) or 29 hours post-fertilisation (hpf) (**B**, **B′**). **A**, **B** Ventral views. **B**, **B′** Lateral views of the same animals.

craniofacial development to our knowledge. Four of the hits we describe (pimozide, retinoic acid, nisoldipine, and leflunomide) were previously reported in a recent screen of zebrafish craniofacial development with a similar design to ours [Kong et al., 2014]. Notably, of the 38 drugs associated with no GFP expression in the primary screen, only 1 drug (leflunomide) was a confirmed hit, and we showed that this compound completely prevented formation of craniofacial cartilage (Fig. 4A).

Temporal and Functional Assessment of Selected Compounds

Representative images of the effects of 4 drug hits on craniofacial cartilage in wild-type embryos are shown in Figure 4. Treatment from mid-to-late epiboly (i.e., "time-zero" in our drug screen) with cyclosporin A, climbazole, or escitalopram caused widening of the ceratohyoids and ceratobranchials and an overall reduction in the lower jaw cartilage, when observed ventrally at 5 dpf (Fig. 4A). In lateral view, the ceratohyoids and Meckel cartilage can be seen to be smaller than in control-treated embryos and downturned (Fig. 4A'). In all 3 cases, the ethmoid cartilage of the upper jaw is present and appeared normal. For each of these drugs, treatment from 29 hpf led to much less severe defects (Fig. 4B, B'). Quantitative increases in the angle between the ceratohyoids in embryos treated from this later time point were most apparent for cyclosporin A. Treatment of embryos with leflunomide from E50 prevented the formation of any cartilage (Fig. 4A), as reported previously [White et al., 2011]. Remarkably, we found that all embryos treated from 29 hpf, after the critical window of NCSC specification and migration [Luo et al., 2001; Carney et al., 2006], were able to form both upper and lower jaw cartilage, although these structures were grossly abnormal (Fig. 4B). This phenotype has not been reported previously and suggests that leflunomide treatment has independent dual effects, inhibiting early NCSC induction and influencing later pharyngeal arch patterning and/or cartilage remodelling. We confirmed that early treatment with leflunomide completely inhibited cranial NCSCs, as demonstrated by in situ hybridisation for *sox10* (see below). Collectively, these results hint at the importance of the timing of drug treatments in relation to formation of NCSC-derived jaw cartilage.

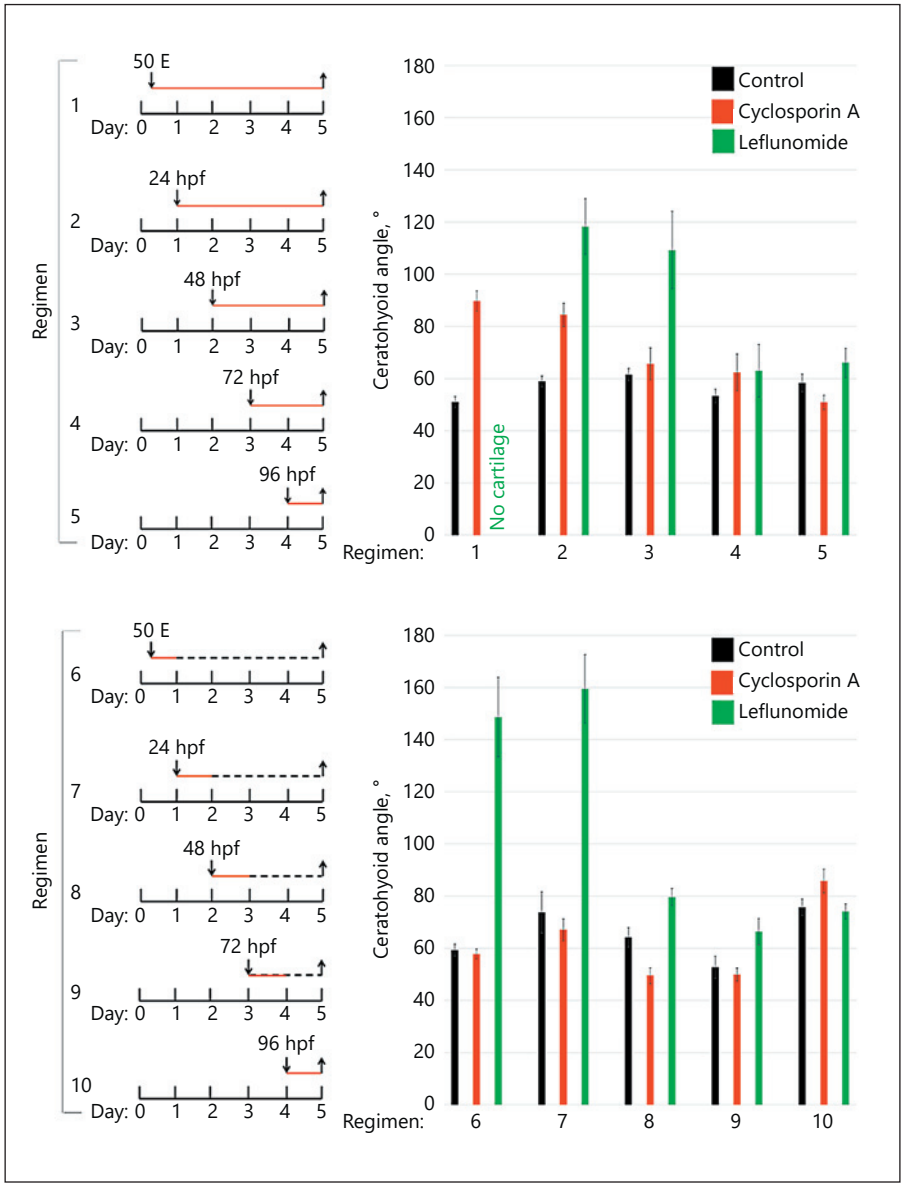

Fig. 5. Temporal effects of leflunomide and cyclosporin A treatment at 5 days post-fertilization. Left: Treatment regimens 1–10 are schematised. ↓: Time point of drug application. Red lines indicate window or drug treatment before either embryo collection or drug washout. ↑: Arrows represent embryo collection. Right: Graphs show angles between ceratohyoid cartilages for each experimental group. Error bars represent standard errors. E, embryonic day; hpf, hours post-fertilization.

Leflunomide is an inhibitor of dihydroorotate dehydrogenase (DHODH), an enzyme that is essential for the production of uracil monophosphate, a constituent base that is integral to ribosomal RNA synthesis and ribosome biogenesis [Trainor and Merrill, 2014]. Cyclosporin A is an inhibitor of calcineurin, which is a calcium-dependent serine/threonine protein phosphatase [Kaminuma, 2008]. In response to increased intracellular calcium, calcineurin dephosphorylates the nuclear factor of T-cells (NFAT) transcription factors, allowing their entry into the cell nucleus where they drive transcription. *Nfatc1*-deficient mice exhibit osteopetrosis within the long bones owing to reduced numbers of bone-resorbing osteoclasts. Importantly in the context of craniosynostosis, they also have fewer osteoblasts and exhibit reduced formation of mineralised bone within the frontal bones of the skull resulting in wider cranial sutures [Winslow et al., 2006]. Given our initial hypothesis that compounds that inhibited either NCSC identities or their differentiation could be candidates for treatment of craniosynostosis, we selected leflunomide and cyclosporin A as representative drugs of each of these categories for further temporal and functional investigations.

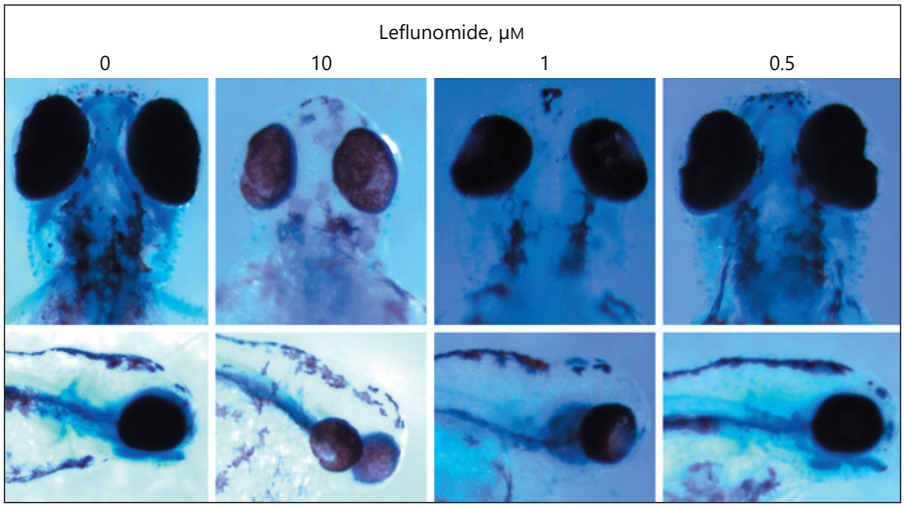

Fig. 6. Dose-response of leflunomide treatment. Representative images in ventral view at 5 days post-fertilization showing effects of indicated doses of leflunomide treatment from 50% epiboly.

We next undertook a full quantitative temporal analysis of the effects of 10 μM doses of these 2 drugs using wild-type embryos stained with Alcian blue. In treatment regimens 1–5, embryos were treated from progressively delayed 24-h time points and visualised at 5 dpf, while in treatment regimens 6–10, embryos were treated during 24-h intervals using drug washout (Fig. 5). The angle of the ceratohyoid cartilage was quantified for approximately 10 zebrafish for each regimen for control- and drug-treated embryos. We noted some variability in this angle in control-treated animals in different clutches of fish, and so we have included this value for matched clutchmate controls for direct comparisons to be made. While leflunomide prevented cartilage formation when applied from E50 (Fig. 4), treatments from either 24 or 48 hpf (regimens 2 and 3) were compatible with jaw cartilage formation but severely enhanced the angle of the ceratohyoid (Fig. 5). By contrast, treatment after 48 hpf had no effect. Interestingly, treatment during day 1 or 2 only (regimens 6 and 7) was compatible with cartilage formation but caused patterning defects of similar magnitude to regimens 2 and 3. Treatment during day 3 caused only subtle patterning defects. Interestingly, we also found that treatment with leflunomide for 5 days did permit formation of cartilage when the dose was diluted by 20-fold, showing that lower doses are consistent with at least partial NCSC induction (Fig. 6). We conclude that leflunomide treatment inhibits cartilage formation during day 1 and disrupts cartilage patterning/differentiation during day 2, but that in both cases, sustained treatment is required to exert these effects. For cyclosporin A, we found that sustained treatment between 2–5 dpf was sufficient to disrupt cartilage, identifying day 2 as the critical effective window, although transient 24-h treatments at any time point were not sufficient to disrupt the lower jaw (Fig. 5). For both drugs, these results identify day 2 as a critical window when the targets of these drugs regulate cartilage patterning/remodelling and suggest that compensatory mechanisms can restore normal cartilage formation if drug treatment is attenuated subsequently.

Finally, to begin to investigate potential cellular and mechanistic targets of these drugs, we performed qRT-PCR on 4-dpf zebrafish treated with 10 μM teriflunomide or FK506 from 29 hpf to monitor markers of key skeletal cell types and cartilage matrix regulatory enzymes using procedures and primers previously reported [Pashay Ahi et al., 2016] (Fig. 7). Teriflunomide treatment reduced expression of the osteoblast marker *spp1* and increased expression of *ctsk* which is expressed in osteoclasts, suggestive of reduced osteoblast and expanded osteoclast cells. Notably, expression of *rankl* which promotes osteoclast formation through paracrine signalling was reduced, which could reflect a feedback mechanism. Teriflunomide also reduced expression of the chondrocyte marker, *col2a1*. Expression of cartilage matrix degrading metalloproteinase enzymes *mmp9* and *mmp13* was increased, while the inhibitor of these enzymes, *timp2a*, was reduced. These findings are consistent with reduction in the jaw cartilage observed following leflunomide/teriflunomide treatment. The same general patterns were observed following FK506 treatment, although the effects were less pronounced. Collectively, these results suggest that drug treatments influence several key skeletogenic cell types and reduce cartilage extracellular matrix.

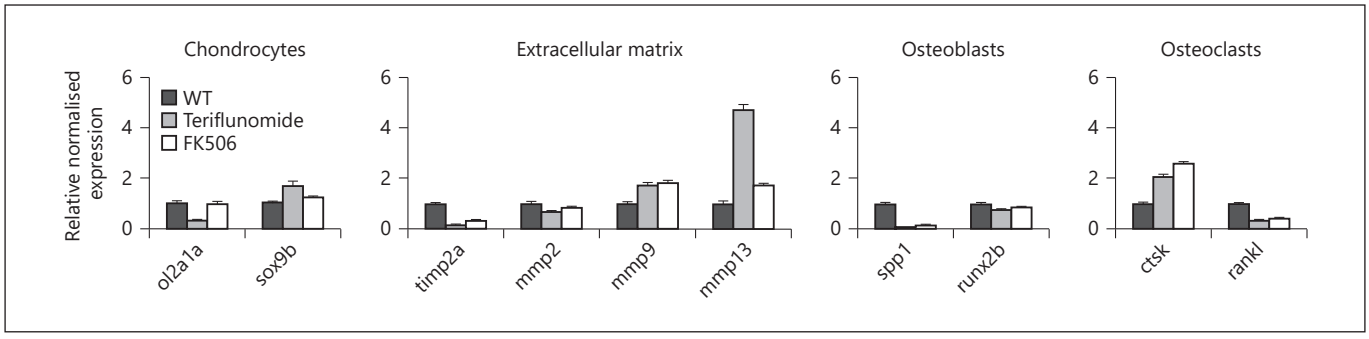

Fig. 7. Effect of drug treatments on skeletogenic gene expression markers. Zebrafish were treated with teriflunomide or FK506, as indicated from 29 hours post-fertilization to 4 days post-fertilization. Error bars are standard errors of the mean. Expression of indicated genes was assessed relative to wild-type (WT) zebrafish treated with DMSO, using primers and procedures as reported previously [Pashay Ahi et al., 2016].

Functional Validation of Leflunomide through Inhibition of NCSC-Derived Neuroblastoma Cells

Perturbation drug screens rely on careful selection of a clinically relevant cell type(s), and because of their disruptive nature, they require subsequent testing in mammalian disease models. To ascertain whether our drug screen could have any relevance to NCSC-related diseases, we began to assess the clinical potential of leflunomide and cyclosporin A in radically different biological settings to the zebrafish jaw.

A first consideration is potential off-target effects of a drug. For this, we tested for phenocopy of the very specific cartilage-loss phenotype associated with leflunomide treatment in zebrafish using a functional analogue. Treatment of embryos with a 10 μM dose of teriflunomide, which is a metabolic derivative of leflunomide, identically reproduced the absence of cartilage formation in all embryos tested (Fig. 8A). Given that this phenotype is consistent with inhibition of NCSC induction, we assessed *sox10* by in situ hybridisation as a marker of endogenous cranial NCSCs. Indeed, leflunomide treatment completely blocked formation of *sox10*+ NCSC formation, although expression within the otic vesicles was preserved, where *sox10* is known to play independent roles in formation of the ear primordium (Fig. 8A). Collectively, these results confirm that DHODH inhibition inhibits NCSC induction.

We next chose to investigate the effects of leflunomide/teriflunomide treatment on human NCSC-derived neuroblastoma cells, as inhibition of NCSC identities in these cells has shown to be of therapeutic value. Specifically, persistent *Sox10* expression has been shown to drive neuroblastoma formation, and depletion of *Sox10* can inhibit NCSC-derived tumour formation [Nagashimada et al., 2012; Shakhova et al., 2012; Kaufman et al., 2016]. We therefore hypothesised that chemical inhibition of DHODH may be therapeutically relevant in neuroblastoma. Treatment of several neuroblastoma cell lines with either leflunomide or teriflunomide caused a dose-dependent reduction in viability (Fig. 8B). By contrast, SK-N-AS cells, which are known to exhibit generalised drug resistance mechanisms [Cohen et al., 1995; Gatsinzi et al., 2012], were more resistant to drug treatment, thereby serving as a control for non-specific toxic effects of the drug. Subsequent to this work, a separate study confirmed our findings, reporting that leflunomide treatment represses neuroblastoma tumour growth in vivo, by inhibiting proliferation, enhancing apoptosis, and inducing S-phase arrest [Zhu et al., 2013]. Therefore, leflunomide is a potential new lead for development of therapeutics in neuroblastoma. Current chemical treatment options for neuroblastoma include application of retinoic acid which induces cellular differentiation and production of dendrites, leading to cellular senescence. In contrast, we found that leflunomide treatment did not cause dendrite production, indicating that this drug works through a distinct mechanism (Fig. 8B).

To gain mechanistic insight into the effects of DHODH inhibition in NCSCs, we used RNAseq to identify global gene expression changes following teriflunomide treatment of SK-N-SH neuroblastoma cells (Fig. 8C) – full dataset given in online supplementary Table 1 (see www.karger.com/doi/10.1159/000491567 for online suppl. material). In total, 133 genes exhibited at >2-fold change in expression levels (adjusted p value <0.05) following 24 h of teriflunomide treatment and were strongly enriched

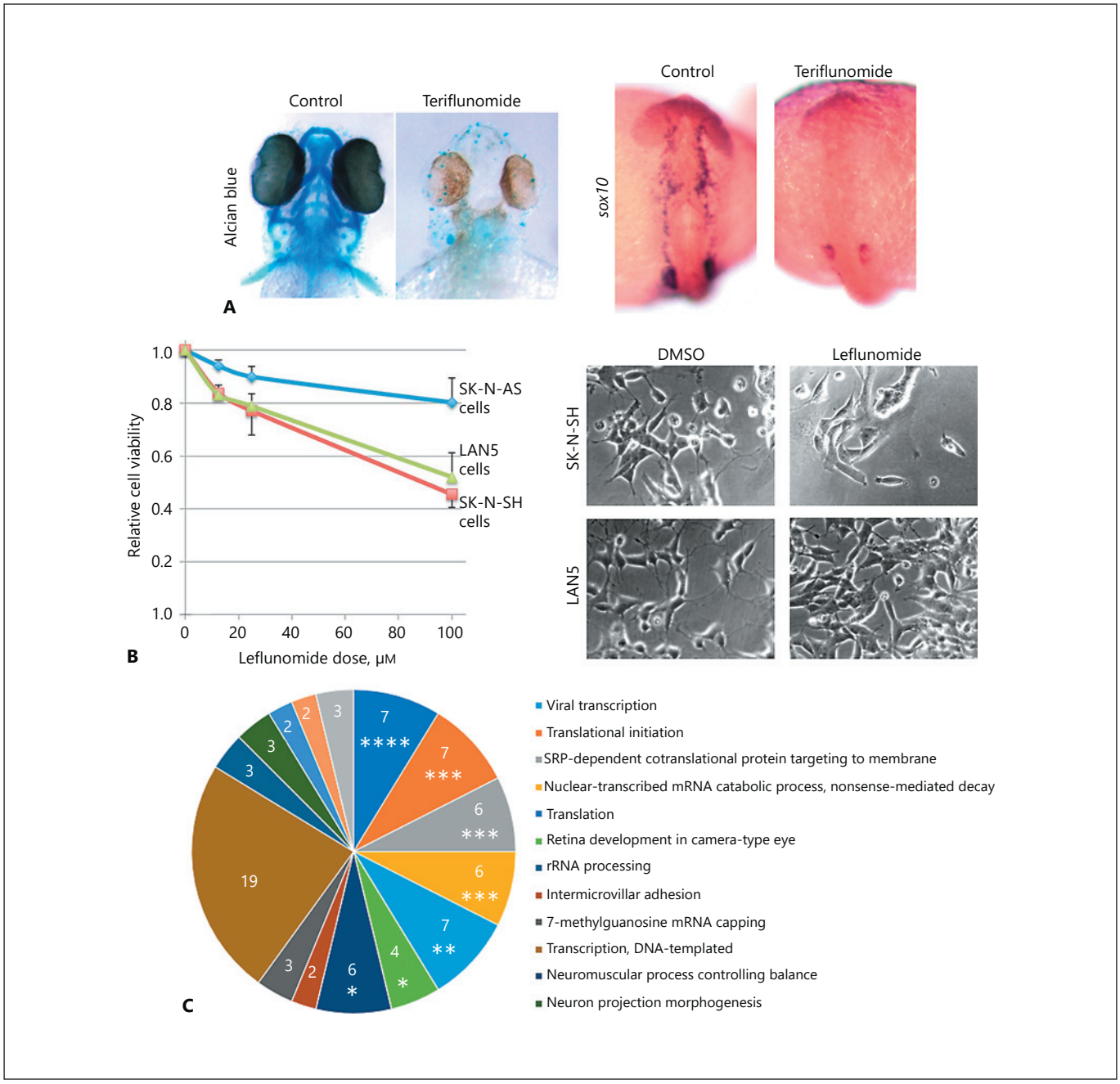

Fig. 8. Functional evaluation of DHODH inhibition. **A** Phenocopy of cartilage-loss phenotype following treatment with 10 μM teriflunomide between 50% epiboly to 5 days post-fertilization, and inhibition of *sox10* expression at 24 hours post-fertilization following teriflunomide treatment, shown by in situ hybridisation. **B** Dose-dependent inhibition of cell numbers in SK-N-SH ($n = 6$), LAN5 ($n = 3$), and SK-N-AS ($n = 5$) cells after 3 days treatment with leflunomide. Data are from CCK8 assays with untreated controls given an arbitrary value of 1. All 100 μM samples are significantly different from untreated samples ($p < 0.05$). Furthermore, at 100 μM both SK-N-SH and LAN5 are significantly more sensitive than SK-N-AS (LAN5:SK-N-AS, $p = 0.025$; SK-N-SH:SK-N-AS, $p = 0.002$; ANOVA with post-hoc Scheffé test). Images show morphology of cells treated with 100 μM leflunomide for 3 days (note no increase in neurite formation, a differentiation marker). **C** Gene ontology terms statistically significantly enriched within the list of differentially expressed genes ($\log_2$-fold change >2, $p < 0.05$) according to DAVID software analysis. Number of terms within each category is listed. **** $p < 5 \times 10^{-5}$; *** $p < 10^{-4}$; ** $p < 10^{-3}$; * $p < 10^{-2}$; no asterisk, $p < 0.05$.

for genes involved in transcription, RNA processing and translation. Consistent with known roles of DHODH in ribosomal RNA synthesis and ribosome biogenesis [Trainor and Merrill, 2014], of 67 downregulated genes with an adjusted p value <0.05, seven (10.4%) encoded ribosomal proteins (of 307 downregulated genes at the less significant p value <0.05 cut-off, 15 (4.9%) encoded ribosomal proteins). In contrast, no ribosomal genes were upregulated, thereby suggesting that leflunomide/teriflunomide inhibit neuroblastoma cell viability through blockade of ribosome biogenesis.

Functional Validation of Tacrolimus as a Potential Therapeutic Compound in Craniosynostosis

FK506 (tacrolimus) is a more potent functional analogue of cyclosporin A. We therefore chose to focus on this drug to evaluate the therapeutic relevance of targeting calcineurin signalling in craniosynostosis. Treatment of zebrafish with 10 μM FK506 from E50 until 5 dpf caused identical jaw cartilage patterning defects that we demonstrated using cyclopsorin A (data not shown), thereby excluding off-target effects as causes of this phenotype.

Given the importance of osteoblasts in craniosynostosis pathogenesis, we began by testing the effect of tacrolimus treatment on primary osteoblasts. Culture of these cells for 14 days led to expression of osteoblast progenitor, pre-osteoblast and mature osteoblast markers, including *Col1a1*, *ALP*, *Runx2*, and *Osx* (Fig. 9A), indicating that this protocol enriched for actively differentiating osteoblasts. These cells were treated with a 10-fold dilution series of FK506 within the range 0–10 μM, which are doses that have previously been shown to correlate with the effects of genetic mutations in *Nfat* genes and are thus likely to be physiologically relevant [Winslow et al., 2006]. Generally, at higher FK506 concentrations, expression of osteoblast differentiation markers was increased compared to control, with the maximal effect generally being achieved at 0.1 μM. We next tested FK506 for rescue of craniosynostosis in a calvarial explant system that we and others have developed using Crouzon mice [Eswarakumar et al., 2006]. Whereas the coronal sutures fused bilaterally over the 2 weeks of culture in all untreated mutant explants, which manifested as a loss of overlap of the frontal and parietal bones and an obliterated suture, none of the FK506-treated mutant explants showed overt signs of fusion after 2 weeks of culture ($p < 0.0001$; Fisher exact test) (Fig. 9B). Quantification of the area of overlap between the frontal and parietal bones for both the left and right coronal sutures demonstrated complete obliteration of this suture in Crouzon mutant calvaria treated with DMSO alone, while there was no difference between Crouzon mutant calvaria treated with FK506 and either treated or untreated wild-type calvaria ($p = 0.530$ and 0.690, respectively; t test) (Fig. 9B). These data provide initial evidence for the therapeutic potential of FK506 in craniosynostosis and supports the need for further in vivo testing.

Discussion

In this study, we undertook a perturbation-based screen of FDA-approved compounds using *sox10:gfp* transgenic zebrafish. This transgene allowed direct visualisation of NCSC-derived craniofacial cartilage that makes up the jaw, without the need for additional staining procedures. We noted partial toxicity of this transgene which manifested as a quantitative increase in the angle between the ceratohyoid cartilages. Thus, it is likely that our screen was sensitised for defects in NCSC-derived craniofacial cartilage. All 14 hits in our screen were reproducible in wild-type/non-transgenic zebrafish confirming that they are not artefacts. Our confirmed drug hit rate was 2.2% of the tested compounds. This is consistent with previously reported perturbation screens [Peterson et al., 2004; Stern et al., 2005; North et al., 2007; Kitambi et al., 2009; Ishizaki et al., 2010; Paik et al., 2010; Rihel et al., 2010; Ni et al., 2011; Peal et al., 2011; Rovira et al., 2011; Namdaran et al., 2012; Ridges et al., 2012; Gut et al., 2013; Le et al., 2013; Kong et al., 2014; Mork and Crump, 2015] suggesting that this screen design had good sensitivity. As discussed in the introduction, while published perturbation screens have an average 29-fold increased hit rate as compared to modifier screens, their success in potential clinical translation is likely to depend on selection of a specific cell type assessed in the screen as well as further testing in mammalian disease models. Repurposing screens using FDA-approved drugs have the advantage that drugs have already passed safety testing in humans. This is important because AstraZeneca reported that data linking a biological target to disease in human subjects and samples were available for 73–82% of the projects that remained active in Phase II, whereas 57–60% of the projects failed on the basis of efficacy where human data was not previously available [Cook et al., 2014].

Our screen focused on NCSC derivatives within the craniofacial cartilage and could therefore identify compounds that regulate NCSCs or remodelling of cartilage/chondrocytes. Since osteoblasts and osteoclasts are also located throughout this cartilage around the time points that we analysed [Eames et al., 2013; Sharif et al., 2014;

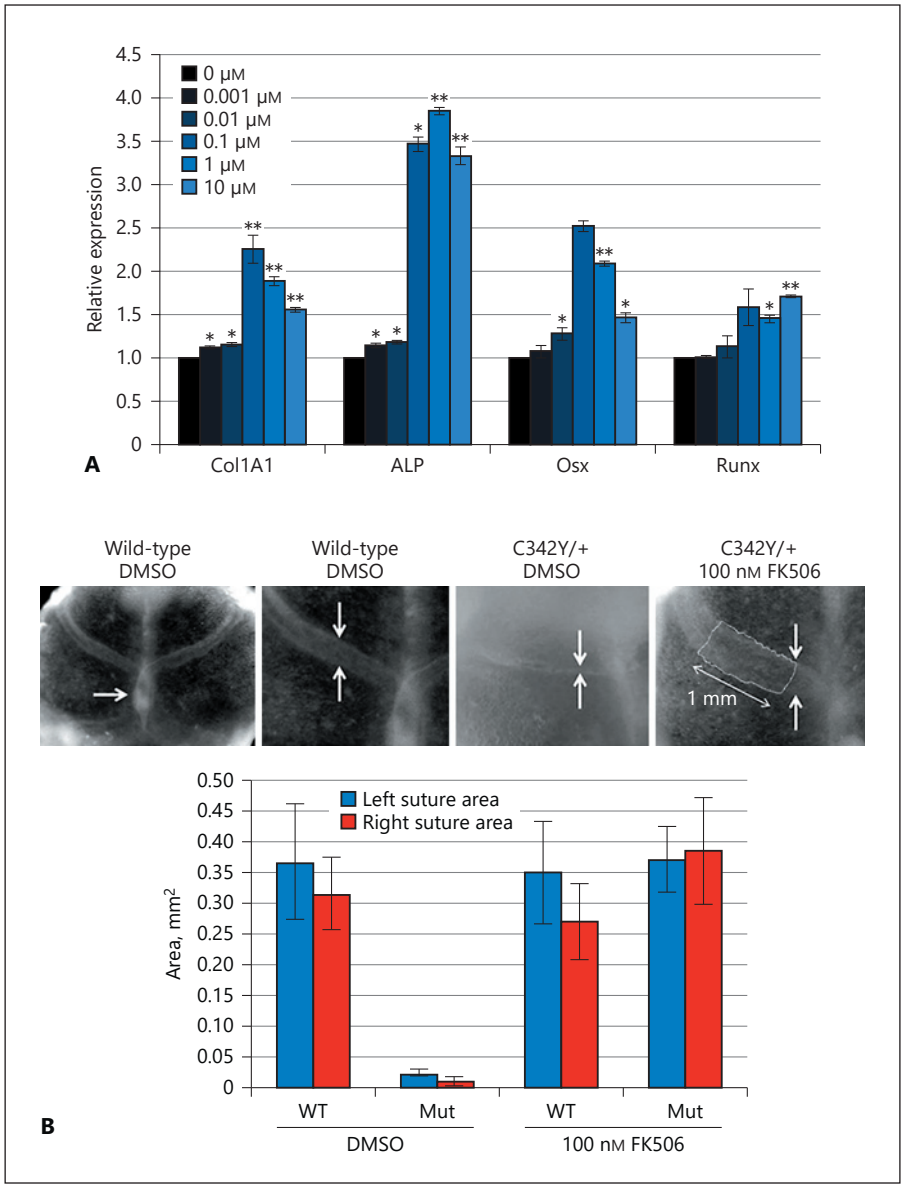

Fig. 9. Functional assessment of calcineurin inhibition in skeletogenesis. **A** Relative expression of osteoblast differentiation marker genes normalised to untreated cells. * $p < 0.05$, ** $p < 0.005$ (t test). **B** E18.5 calvarial explants cultured for 2 weeks in the presence or absence of 100 nM FK506. Top row: Low-power view of a control explant; note overlap of the midline parietal bones (arrows), showing continued osteogenesis of the sutures (1st and 2nd images). Whereas the DMSO-treated C342Y/+ coronal sutures undergo synostosis, FK506-treated C342Y/+ explants do not (arrows, 3rd and 4th images). The last image shows how the area of overlap of the frontal and parietal bones was measured over a fixed 1-mm length of suture (outlined) to gain a robust measure of suture width. These values are summarised over 33 explants, either wild-type (WT) or mutant (Mut), treated with DMSO or FK506. Values are given for both the left and right sutures for each explant.

Mork and Crump, 2015], it is conceivable that our screen could also identify compounds that influence these cell types, although we note that no mineralised bone is present at these stages. Indeed, our temporal analyses of leflunomide treatment suggested biphasic effects in repressing early NCSC induction and later independent effects on cartilage remodelling. By contrast, our temporal analyses of other drug hits, including cyclosporin A, supported roles limited to cartilage remodelling. For both drugs, our data suggested that sustained drug treatments are also important to reproduce jaw patterning defects, which raises the possibility that compensatory mechanisms can restore normal formation of the jaw. In future, it will be interesting to characterise the exact cellular targets of these drugs as well as drug treatment timing and duration when considering possible clinical application (e.g., craniosynostosis). For both drugs, we were also able to generate initial ex vivo data suggesting their potential relevance for treatment of neuroblastoma or craniosynostosis in mammalian systems. While these data provide some proof-of-concept support for our drug screen, it will be necessary to undertake further pre-clinical testing in precise in vivo models of disease treatment, and this will form the subject of future reports.

Table 1. List of drug hits, description and evidence supporting links to osteoarthritis pathogenesis and bone mineral density reduction in humans

Drug	Target	Biochemical/cellular targets	Evidence that this compound reduces bone mineral density in humans[a]	Evidence for relevance to OA
Novel hits				
Vinorelbine	Anti-mitotic/chemotherapy	Mitosis, tubulin	No	–
Cyclosporin A	Calcineurin inhibitor	pCaN; pNFAT; couples to AP-1 transcription factor involving cJun	Yes	Calcineurin participates in the progression of OA, and mice lacking the downstream transcription factor, *Nfatc2*, exhibit joint degradation and abnormal chondrocyte anabolism/catabolism [Yoo et al., 2007; Wang et al., 2009; Beier, 2014]
Nicardipine HCl	L-type Ca2+ channel blocker		No	L-type Ca^{2+} channel blocker, verapamil, protects against OA [Takamatsu et al., 2014]
Climbazole	Anti-fungal		No	–
Clomiphene	Selective oestrogen receptor modulator	Oestrogen receptors translocate to the nucleus acting as transcription factors	Yes	Oestrogen receptor polymorphisms are associated with OA risk and oestrogen may account for higher OA incidence in women [Bay-Jensen et al., 2013; Yin et al., 2015]
Adapalene	Retinoid	Possible control of transcription through retinoic acid receptors	Yes	RA ligands are elevated in OA and induce ADAM28 expression and proteoglycan degradation in chondrocytes [Davies et al., 2009; Hikichi et al., 2009]
Entacapone	COMT inhibitor (dopaminergic neurons)	Degrades catecholamines (e.g., dopamine)	No	Increased expression of dopamine receptors in synovial fibroblasts in rheumatoid arthritis [Capellino et al., 2014]
Amoxapine	Serotonin/epinephrine re-uptake inhibitor	Increases ligand upstream of PKC	Yes	–
Escitalopram	Selective serotonin re-uptake inhibitor	Increases ligand upstream of PKC	Yes	–
Nisoldipine	Calcium channel blocker	Upstream of CaN and NFAT	Yes	L-type Ca^{2+} channel blocker, verapamil, protects against OA [Takamatsu et al., 2014]
Known hits				
Leflunomide	DHODH inhibitor	DHODH	No	–
Retinoic acid	Retinoic acid signalling	Possible control of transcription through retinoic acid receptors	Yes	RA ligands are elevated in OA and induce ADAM28 expression and proteoglycan degradation in chondrocytes [Davies et al., 2009; Hikichi et al., 2009]
Diazoxide	Potassium channel activator	Electrochemical signalling	No	Potassium channels are expressed in articular chondrocytes [Mobasheri et al., 2007]
Pimozide	Anti-psychotic		No	–
Functional analogues				
Tacrolimus (FK506)	Calcineurin inhibitor	pCaN; pNFAT; couples to AP-1 transcription factor involving cJun	Yes	Calcineurin participates in the progression of OA, and mice lacking the downstream transcription factor, *Nfatc2*, exhibit joint degradation and abnormal chondrocyte anabolism/catabolism [Yoo et al., 2007; Wang et al., 2009; Beier, 2014]
Teriflunomide	Metabolic derivative of leflunomide	DHODH	No	–

DHODH, dehydroorotate dehydrogenase; OA, osteoarthritis. [a] Capellino et al., 2014.

Of our drug hits, 50–64% are known to target pathways implicated in osteoarthritis (OA) pathogenesis or regulation of bone mineral density (Table 1) [Mazziotti et al., 2010], and at least 1 drug disrupted early NCSC development. This likely reflects the design of our screen which visualised patterning of NCSC-derived skeletal elements. Thus, the hits that we report could be relevant to skeletal tissue homeostasis and disease in a number of different contexts and emphasise the transferability of the perturbation screen design when focused on a specific cell/tissue type of medical relevance. Chondrocytes represent a key cellular component of articular cartilage which is affected in all joints with OA [Buckwalter et al., 2005]. Changes within the microenvironment of the joint can induce an inflammatory response, whereby chondrocytes release cytokines (e.g., IL1β) and matrix-degrading enzymes. Joint destabilisation can lead to increased expression of metalloproteinases, such as AD-

AMTS5 and MMP13, which are downregulated following joint immobilisation [Burleigh et al., 2012]. Several known human OA susceptibility genes, including *gdf5* and *mcf2l*, are expressed in zebrafish craniofacial cartilage elements and joints from just a few dpf [Mitchell et al., 2013]. Analysis of zebrafish cartilage is therefore directly relevant to OA of the temporomandibular joint which affects approximately 17% of the OA patients [Gremillion et al., 1993].

The drug hits fall into several functional categories, including calcium, retinoic acid receptor, oestrogen, and neuropeptide signalling pathways (Table 1). Leflunomide was the only compound for which we demonstrate clear evidence for direct effects on NCSCs, and this drug has previously been shown to inhibit $BRAF^{V600E}$-driven melanoma cell growth, which has been proposed to reflect suppression of NCSC identities [White et al., 2011]. Our RNAseq data in neuroblastoma cells suggested that DHODH inhibition particularly affected ribosomal gene expression and transcription. NCSC-derived neuroblastoma cells are known to activate expression of ribosomal genes such that protein synthesis can keep pace with the demands of increased proliferation. This is driven by the protooncogene, *MYCN* [Boon et al., 2001], which is commonly activated in neuroblastoma.

Cyclosporin A and FK506 are inhibitors of calcineurin, which is a calcium-dependent serine/threonine protein phosphatase [Kaminuma, 2008]. In response to increased intracellular calcium, calcineurin dephosphorylates the NFAT transcription factors, allowing their entry into the cell nucleus where they drive transcription. *Nfatc1*-deficient mice exhibit osteopetrosis within the long bones owing to reduced numbers of bone-resorbing osteoclasts. They also have fewer osteoblasts and exhibit reduced formation of mineralized bone within the frontal bones of the skull resulting in wider cranial sutures [Winslow et al., 2006]. Similar effects on osteoblast and osteoclast cell lineages have been observed in calcineurin β1 mutant mice. Calcineurin β1 [Cnb1, also known as Ppp3r1, protein phosphatase 3, regulatory subunit B, alpha isoform (calcineurin B, type I)] is a Ca^{2+}-binding regulatory subunit of heterodimeric calcineurin. Loss of the Cnb1 subunit results in a lack of calcineurin enzymatic activity in non-germline cell types. Conditionally targeted mutant mice whereby the *Cnb1* gene was inactivated in osteoblasts increased bone mineral density, associated with increased differentiation and mineralisation of primary calvarial osteoblast cultures, and failure of these osteoblasts to support osteoclast growth and survival [Winslow et al., 2006].

These observations led us to hypothesise that FK506 treatment could prevent cranial suture fusion in Crouzon syndrome mice, and we generated initial support for this idea using a calvarial explant system. To take this observation further in future, it will be necessary to test the drug in vivo, evaluate systems for localised drug delivery to avoid unwanted side effects, and to characterise the key skeletal cell type(s) that are influenced within the calvarium since calcineurin signalling can influence osteoblast and osteoclast cells and precursors. Of note, this compound is approved for long-term immunosuppression of very young babies who undergo organ transplantation, suggesting that it may also be efficacious for treatment of craniosynostosis over the first few years of life.

In summary, the identification of new chemical structures that influence NCSC-derived skeletal structures provides new insight into global mechanisms of skeletogenesis and provides a basis to begin to explore possible treatments for conditions such as craniosynostosis. We add to the growing literature concerning use of zebrafish as an in vivo system for chemical screening, which is an important application of this model organism. In future, it will be necessary to characterise these and other drug hits that regulate craniofacial development, including the particular target cell lineages and the utility of these compounds in mammalian disease models.

Acknowledgements

This work was funded by a Medical Research Council New Investigator Research Grant (MR/L009978/1) and Action Medical Research Project Grant (GN2595) to D.J. This research was also supported by the National Institute for Health Research Biomedical Research Centre at Great Ormond Street Hospital for Children NHS Foundation Trust and University College London.

Statement of Ethics

Procedures involving animals were performed in accordance with Home Office guidelines (PPL 70/7892).

Disclosure Statement

The authors have no conflicts of interest to disclose.

References

Aberg T, Rice R, Rice D, Thesleff I, Waltimo-Sirén J: Chondrogenic potential of mouse calvarial mesenchyme. J Histochem Cytochem 53: 653–663 (2005).

Babbs C, Stewart HS, Williams LJ, Connell L, Goriely A, et al: Duplication of the *EFNB1* gene in familial hypertelorism: imbalance in ephrin-B1 expression and abnormal phenotypes in humans and mice. Hum Mutat 32: 930–938 (2011).

Bay-Jensen AC, Slagboom E, Chen-An P, Alexandersen P, Qvist P, et al: Role of hormones in cartilage and joint metabolism: understanding an unhealthy metabolic phenotype in osteoarthritis. Menopause 20:578–586 (2013).

Beier F: NFATs are good for your cartilage! Osteoarthritis Cartilage 22:893–895 (2014).

Boon K, Caron HN, van Asperen R, Valentijn L, Hermus MC, et al: N-myc enhances the expression of a large set of genes functioning in ribosome biogenesis and protein synthesis. EMBO J 20:1383–1393 (2001).

Buckwalter JA, Mankin HJ, Grodzinsky AJ: Articular cartilage and osteoarthritis. Instr Course Lect 54:465–480 (2005).

Burleigh A, Chanalaris A, Gardiner MD, Driscoll C, Boruc O, et al: Joint immobilization prevents murine osteoarthritis and reveals the highly mechanosensitive nature of protease expression in vivo. Arthritis Rheum 64:2278–2288 (2012).

Capellino S, Cosentino M, Luini A, Bombelli R, Lowin T, et al: Increased expression of dopamine receptors in synovial fibroblasts from patients with rheumatoid arthritis: inhibitory effects of dopamine on interleukin-8 and interleukin-6. Arthritis Rheumatol 66:2685–2693 (2014).

Carney TJ, Dutton KA, Greenhill E, Delfino-Machín M, Dufourcq P, et al: A direct role for *Sox10* in specification of neural crest-derived sensory neurons. Development 133:4619–4630 (2006).

Cheng S, Kesavan C, Mohan S, Qin X, Alarcon CM, et al: Transgenic overexpression of ephrin b1 in bone cells promotes bone formation and an anabolic response to mechanical loading in mice. PLoS One 8:e69051 (2013).

Cohen PS, Letterio JJ, Gaetano C, Chan J, Matsumoto K, et al: Induction of transforming growth factor beta 1 and its receptors during all-trans-retinoic acid (RA) treatment of RA-responsive human neuroblastoma cell lines. Cancer Res 55:2380–2386 (1995).

Cook D, Brown D, Alexander R, March R, Morgan P, et al: Lessons learned from the fate of AstraZeneca's drug pipeline: a five-dimensional framework. Nat Rev Drug Discov 13: 419–431 (2014).

Davies MR, Ribeiro LR, Downey-Jones M, Needham MR, Oakley C, Wardale J: Ligands for retinoic acid receptors are elevated in osteoarthritis and may contribute to pathologic processes in the osteoarthritic joint. Arthritis Rheum 60:1722–1732 (2009).

Deckelbaum RA, Holmes G, Zhao Z, Tong C, Basilico C, Loomis CA: Regulation of cranial morphogenesis and cell fate at the neural crest-mesoderm boundary by engrailed 1. Development 139:1346–1358 (2012).

Dutton JR, Antonellis A, Carney TJ, Rodrigues FS, Pavan WJ, et al: An evolutionarily conserved intronic region controls the spatiotemporal expression of the transcription factor Sox10. BMC Dev Biol 8:105 (2008).

Eames BF, DeLaurier A, Ullmann B, Huycke TR, Nichols JT, et al: FishFace: interactive atlas of zebrafish craniofacial development at cellular resolution. BMC Dev Biol 13:23 (2013).

Eswarakumar VP, Ozcan F, Lew ED, Bae JH, Tomé F, et al: Attenuation of signaling pathways stimulated by pathologically activated FGF-receptor 2 mutants prevents craniosynostosis. Proc Natl Acad Sci USA 103:18603–18608 (2006).

Gatsinzi T, Ivanova EV, Iverfeldt K: TRAIL resistance in human neuroblastoma SK-N-AS cells is dependent on protein kinase C and involvesinhibition of caspase-3 proteolytic processing. J Neurooncol 109:503–512 (2012).

Gremillion H, Bates R, Stewart C: Degenerative joint disease. Part I: diagnosis and management considerations. Cranio 11:284–290 (1993).

Gut P, Baeza-Raja B, Andersson O, Hasenkamp L, Hsiao J, et al: Whole-organism screening for gluconeogenesis identifies activators of fasting metabolism. Nat Chem Biol 9:97–104 (2013).

Hehr U, Muenke M: Craniosynostosis syndromes: from genes to premature fusion of skull bones. Mol Genet Metab 68:139–151 (1999).

Hikichi Y, Yoshimura K, Takigawa M: All-trans retinoic acid-induced ADAM28 degrades proteoglycans in human chondrocytes. Biochem Biophys Res Commun 386:294–299 (2009).

Ishizaki H, Spitzer M, Wildenhain J, Anastasaki C, Zeng Z, et al: Combined zebrafish-yeast chemical-genetic screens reveal gene-copper-nutrition interactions that modulate melanocyte pigmentation. Dis Model Mech 3:639–651 (2010).

Jiang X, Iseki S, Maxson RE, Sucov HM, Morriss-Kay GM: Tissue origins and interactions in the mammalian skull vault. Dev Biol 241:106–116 (2002).

Kaminuma O: Selective inhibitors of nuclear factor of activated T cells: potential therapeutic drugs for the treatment of immunological and inflammatory diseases. Inflamm Allergy Drug Targets 7:35–40 (2008).

Kaufman CK, Mosimann C, Fan ZP, Yang S, Thomas AJ, et al: A zebrafish melanoma model reveals emergence of neural crest identity during melanoma initiation. Science 351: aad2197 (2016).

Keupp K, Li Y, Vargel I, Hoischen A, Richardson R, et al: Mutations in the interleukin receptor *IL11RA* cause autosomal recessive Crouzon-like craniosynostosis. Mol Genet Genomic Med 1:223–237 (2013).

Kitambi SS, McCulloch KJ, Peterson RT, Malicki JJ: Small molecule screen for compounds that affect vascular development in the zebrafish retina. Mech Dev 126:464–477 (2009).

Kong Y, Grimaldi M, Curtin E, Dougherty M, Kaufman C, et al: Neural crest development and craniofacial morphogenesis is coordinated by nitric oxide and histone acetylation. Chem Biol 21:488–501 (2014).

Le X, Pugach EK, Hettmer S, Storer NY, Liu J, et al: A novel chemical screening strategy in zebrafish identifies common pathways in embryogenesis and rhabdomyosarcoma development. Development 140:2354–2364 (2013).

Luo R, An M, Arduini BL, Henion PD: Specific pan-neural crest expression of zebrafish Crestin throughout embryonic development. Dev Dyn 220:169–174 (2001).

Mazziotti G, Canalis E, Giustina A: Drug-induced osteoporosis: mechanisms and clinical implications. Am J Med 123:877–884 (2010).

Merrill AE, Bochukova EG, Brugger SM, Ishii M, Pilz DT, et al: Cell mixing at a neural crest-mesoderm boundary and deficient ephrin-Eph signaling in the pathogenesis of craniosynostosis. Hum Mol Genet 15:1319–1328 (2006).

Mitchell RE, Huitema LF, Skinner RE, Brunt LH, Severn C, et al: New tools for studying osteoarthritis genetics in zebrafish. Osteoarthritis Cartilage 21:269–278 (2013).

Mobasheri A, Gent TC, Nash AI, Womack MD, Moskaluk CA, Barrett-Jolley R: Evidence for functional ATP-sensitive (K_{ATP}) potassium channels in human and equine articular chondrocytes. Osteoarthritis Cartilage 15:1–8 (2007).

Mork L, Crump G: Zebrafish craniofacial development: a window into early patterning. Curr Top Dev Biol 115:235–269 (2015).

Nagashimada M, Ohta H, Li C, Nakao K, Uesaka T, et al: Autonomic neurocristopathy-associated mutations in PHOX2B dysregulate *Sox10* expression. J Clin Invest 122:3145–3158 (2012).

Namdaran P, Reinhart KE, Owens KN, Raible DW, Rubel EW: Identification of modulators of hair cell regeneration in the zebrafish lateral line. J Neurosci 32:3516–3528 (2012).

Ni TT, Rellinger EJ, Mukherjee A, Xie S, Stephens L, et al: Discovering small molecules that promote cardiomyocyte generation by modulating Wnt signaling. Chem Biol 18:1658–1668 (2011).

Nieminen P, Morgan NV, Fenwick AL, Parmanen S, Veistinen L, et al: Inactivation of IL11 signaling causes craniosynostosis, delayed tooth eruption, and supernumerary teeth. Am J Hum Genet 89:67–81 (2011).

North TE, Goessling W, Walkley CR, Lengerke C, Kopani KR, et al: Prostaglandin E2 regulates vertebrate haematopoietic stem cell homeostasis. Nature 447:1007–1011 (2007).
Paik EJ, de Jong JL, Pugach E, Opara P, Zon LI: A chemical genetic screen in zebrafish for pathways interacting with *cdx4* in primitive hematopoiesis. Zebrafish 7:61–68 (2010).
Pashay Ahi EP, Walker BS, Lassiter CS, Jónsson ZO: Investigation of the effects of estrogen on skeletal gene expression during zebrafish larval head development. Peer J 4:e1878 (2016).
Peal DS, Mills RW, Lynch SN, Mosley JM, Lim E, et al: Novel chemical suppressors of long QT syndrome identified by an in vivo functional screen. Circulation 123:23–30 (2011).
Peterson RT, Shaw SY, Peterson TA, Milan DJ, Zhong TP, et al: Chemical suppression of a genetic mutation in a zebrafish model of aortic coarctation. Nat Biotechnol 22:595–599 (2004).
Rennekamp AJ, Peterson RT: 15 years of zebrafish chemical screening. Curr Opin Chem Biol 24: 58–70 (2015).
Ridges S, Heaton WL, Joshi D, Choi H, Eiring A, et al: Zebrafish screen identifies novel compound with selective toxicity against leukemia. Blood 119:5621–5631 (2012).
Rihel J, Prober DA, Arvanites A, Lam K, Zimmerman S, et al: Zebrafish behavioral profiling links drugs to biological targets and rest/wake regulation. Science 327:348–351 (2010).
Rovira M, Huang W, Yusuff S, Shim JS, Ferrante AA, et al: Chemical screen identifies FDA-approved drugs and target pathways that induce precocious pancreatic endocrine differentiation. Proc Natl Acad Sci USA 108:19264–19269 (2011).
Schilling TF, Kimmel CB: Musculoskeletal patterning in the pharyngeal segments of the zebrafish embryo. Development 124:2945–2960 (1997).
Schwerd T, Twigg SRF, Aschenbrenner D, Manrique S, Miller KA, et al: A biallelic mutation in *IL6ST* encoding the GP130 co-receptor causes immunodeficiency and craniosynostosis. J Exp Med 214:2547–2562 (2017).
Shakhova O, Zingg D, Schaefer SM, Hari L, Civenni G, et al: *Sox10* promotes the formation and maintenance of giant congenital naevi and melanoma. Nat Cell Biol 14:882–890 (2012).
Sharif F, de Bakker MA, Richardson MK: Osteoclast-like cells in early zebrafish embryos. Cell J 16:211–224 (2014).
Stern HM, Murphey RD, Shepard JL, Amatruda JF, Straub CT, et al: Small molecules that delay S phase suppress a zebrafish bmyb mutant. Nat Chem Biol 1:366–370 (2005).
Takamatsu A, Ohkawara B, Ito M, Masuda A, Sakai T, et al: Verapamil protects against cartilage degradation in osteoarthritis by inhibiting Wnt/β-catenin signaling. PLoS One 9: e92699 (2014).
Trainor PA, Merrill AE: Ribosome biogenesis in skeletal development and the pathogenesis of skeletal disorders. Biochim Biophys Acta 1842:769–778 (2014).
Twigg SR, Wilkie AO: A genetic-pathophysiological framework for craniosynostosis. Am J Hum Genet 97:359–377 (2015).
Twigg SR, Kan R, Babbs C, Bochukova EG, Robertson SP, et al: Mutations of ephrin-B1 (*EFNB1*), a marker of tissue boundary formation, cause craniofrontonasal syndrome. Proc Natl Acad Sci USA 101:8652–8657 (2004).
Twigg SR, Matsumoto K, Kidd AM, Goriely A, Taylor IB, et al: The origin of *EFNB1* mutations in craniofrontonasal syndrome: frequent somatic mosaicism and explanation of the paucity of carrier males. Am J Hum Genet 78:999–1010 (2006).
Twigg SR, Babbs C, van den Elzen ME, Goriely A, Taylor S, et al: Cellular interference in craniofrontonasal syndrome: males mosaic for mutations in the X-linked *EFNB1* gene are more severely affected than true hemizygotes. Hum Mol Genet 22:1654–1662 (2013).
Wang J, Gardner BM, Lu Q, Rodova M, Woodbury BG, et al: Transcription factor Nfat1 deficiency causes osteoarthritis through dysfunction of adult articular chondrocytes. J Pathol 219:163–172 (2009).
White RM, Cech J, Ratanasirintrawoot S, Lin CY, Rahl PB, et al: DHODH modulates transcriptional elongation in the neural crest and melanoma. Nature 471:518–522 (2011).
Wiley DS, Redfield SE, Zon LI: Chemical screening in zebrafish for novel biological and therapeutic discovery. Methods Cell Biol 138: 651–679 (2017).
Wilkie AO, Byren JC, Hurst JA, Jayamohan J, Johnson D, et al: Prevalence and complications of single-gene and chromosomal disorders in craniosynostosis. Pediatrics 126:e391–400 (2010).
Winslow MM, Pan M, Starbuck M, Gallo EM, Deng L, et al: Calcineurin/NFAT signaling in osteoblasts regulates bone mass. Dev Cell 10: 771–782 (2006).
Yin YW, Sun QQ, Hu AM, Wang Q, Liu HL: Association of rs9340799 polymorphism in estrogen receptor alpha gene with the risk ofosteoarthritis: evidence based on 8,792 subjects. Mol Genet Genomics 290:513–520 (2015).
Yoo SA, Park BH, Yoon HJ, Lee JY, Song JH, et al: Calcineurin modulates the catabolic and anabolic activity of chondrocytes and participates in the progression of experimental osteoarthritis. Arthritis Rheum 56:2299–2311 (2007).
Zhu S, Yan X, Xiang Z, Ding HF, Cui H: Leflunomide reduces proliferation and induces apoptosis in neuroblastoma cells in vitro and in vivo. PLoS One 8:e71555 (2013).